Uniaxial Compression Tests: Machine Development and Application to Metals and Metal Alloys

Pedro M.G. Santos
pedromgsantos@tecnico.ulisboa.pt

Instituto Superior Técnico, Universidade de Lisboa, Portugal
May 2019

Abstract

This research presents the development of a testing machine, for uniaxial compression of small test specimens. The validation of the experimental apparatus was based on experimental results described in the literature. Further on, tests were carried out to evaluate the mechanical behavior of pure metals and metal alloys using the specially designed testing machine. The findings shown that the material hardness and the flow stress are influenced by the strain and the strain rate.

Keywords: Mechanical characterization, metals, uniaxial compression, strain rate, flow stress, material hardness.

1. Introduction

Nowadays, in order to meet all the customer's needs, it is necessary that the companies bear in mind some important aspects regarding the production of products, such as the properties of the materials used in its production. Thus, the mechanical characterization of materials assumes a fundamental relevance in the manufacturing processes, since it allows to expose the relation between stress, strain and strain rates to which the materials are subjected to in the manufacturing processes.

There are reports in the literature that suggest that the strain rates obtained in the mechanical tests do not replicate the plastic flow neither the strain rates that are practiced in the manufacturing processes (Guo 2003). This reality brings up the necessity of establishing the deformation conditions of the material during the manufacturing process for an appropriate choice of the mechanical test (Lei et al.,1999).

The strain rate, which is expressed in units s^{-1} and is given by the following expression:

$$\dot{\varepsilon} = \frac{d\varepsilon}{dt} \quad (1)$$

There is a set of mechanical tests that allows us to study the mechanical behavior of materials. This set of tests is different depending on the time of application of the load and on the strain rate imposed on the material. For quasi-static loading conditions (10^{-4}-1 s^{-1}), the mechanical characterization is usually made using machines for compression, torsion, and other processes. For medium strain rates (1-10^2 s^{-1}), equipment based on drop hammer, hydraulic systems, or mechanical systems are generally used. For high strain rates (> 10^2 s^{-1}), Hopkinson bar-type equipment or Taylor impact devices are typically used.

The goal of the present investigation is to study the mechanical behavior of pure

metals and metal alloys when subjected to strain rates ranging from 0.1 s^{-1} to 3 s^{-1}. In order to achieve this, it was necessary: (i) to prepare a machine capable of compressing specimens; (ii) to develop suitable sensors to monitor test parameters; and (iii) to develop a programming code that registers the parameters obtained in the test. The study of the mechanical behavior of the materials was carried out through uniaxial compression tests with different strain rates and through a Vickers hardness study.

For the compression tests, the true stress is calculated through:

$$\sigma = \frac{F}{A_i} \tag{2}$$

Where F is the force applied on the specimen and A_i is the instantaneous area of the specimen. Through the condition of incompressibility, the instantaneous area of the specimen is calculated from the following expression:

$$A_i = \frac{V}{h_i} = \frac{A_0 h_0}{h_i} = \frac{\pi \left(\frac{\emptyset_0}{2}\right)^2 h_0}{h_0 - d} \tag{3}$$

Where V is the volume of the specimen, h_i is the height of the specimen at a given time, h_0 is the initial height of the specimen, $\emptyset_0$ is the initial diameter of the specimen and d is the displacement.

The true strain, ε is calculated through:

$$\varepsilon = -\int_{h_0}^{h_i} \frac{dh}{h} = \ln \frac{h_0}{h_i} \tag{4}$$

For the hardness tests, the Vickers hardness number is achieved by the following expression:

$$HV = 1.854 \frac{P}{d^2} \tag{5}$$

2. Development of experimental apparatus

2.1. Test Machine

In order to perform the compression tests, a press was used containing a mechanism Crank-Connecting Rod system.

2.2. Uniaxial Compression Tool

In order to carry out the tests, a compression tool was developed to compress small size specimens. The production of the compression tool was done aiming the absence of any gaps or vibrations that could compromise the results of this investigation. In figure 1 is presented the CAD model of the tool and the components that were designed. The tool includes mechanical components that ensure the parallelism of the compression plates and sensors that allow the monitoring of the physical parameters (force and displacement) of the compression test. As regards to compression plates, these are the most important components of the tool, since they must withstand all the effort involved in the compression of the specimens. Thereby, from a study developed Afonso Gregorio (2017), it was decided to manufacture compression plates (4) in hard metal (tungsten carbide) using wire electro-erosion and grinding processes.

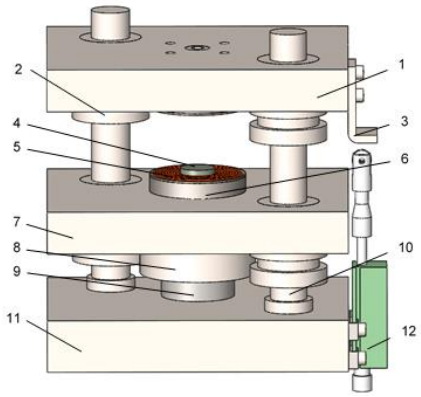

*Figure 1. Compression tool: **1 -** Top platen; **2 -** Bushings; **3 -** Actuator; **4 -** Compression Platen; **5 -** Displacement Sensor; **6 -** Platen; **7 -** Bottom platen; **8 -** Load cell help part; **9 -**Load cell; **10 -** Guide; **11 -** Tool Base; **12 -** Commercial Displacement Sensor.*

2.3. Instrumentation and Data Acquisition

The tool's instrumentation includes a load cell which measures the compressive force and two displacement sensors that measure the relative distance between the compression plates.

Load Cell

The compressive force is monitored by a 5-tonne DYHW-16, DAYSENSOR commercial load cell (figure 2). This load contains four resistance strain gauges coupled to a Wheatstone bridge circuit

Figure 2.Load Cell.

Since the voltage value sent by the load cell is very low, the load cell was connected to an amplification and signal conditioning system. The amplifier used was from the manufacturer CALT, model JY-S60. The sensitivity of the load cell is 2 mV per V of excitation, and the amplifier has 10V as its maximum excitation value. Therefore, when the load cell is subjected to the maximum load it will have a response of 20 mV. The calibration curve of the load cell was made using calibrated weights, making a relation between the value of the weights calibrated with the voltage value obtained the amplifier.

Displacement Sensors

To obtain the relative distance between the compressor plates two displacement sensors were used: (i) a commercial displacement sensor (see figure 3 (a)) and (ii) a sensor developed to capture displacements with the greatest possible sensitivity (see figure 3 (b)).

(a) (b)

Figure 3. Displacement Sensors.

Sensors Developed

The sensors developed are based on the principle of electromagnetic induction between coils, *i.e.*, the current imposed on a coil occurs the generation of an electromagnetic field that will induce an electric current in the opposite coil. This current varies with the distance to which the two coils meet one another. Based on this concept, the resulting voltage on the receiver coil enable to know the distance in which the two coils are located, keeping the voltage signal of the transmitter coil constant. The advantage of this type of sensors when compared to commercial displacement sensor is the accuracy of the measurement, since the assembly of this type of sensors avoids undesirable contributions coming from the elastic deformation of the tool during the entire test.

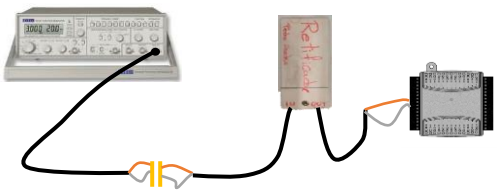

Figure 4. Schematic representation of the process acquiring distance between sensors developed.

For the emission of the signal in the coils it was used the TG315 function generator of AIM & TTi. (figure 4). Since the signal emitted by the function generator is an AC signal and the data acquisition board receives only DC signals, this signal needed to be rectified to a DC signal. Thus, a rectifier was developed, consisting of a 4-semiconductor diode rectifier bridge in silicon (figure 5).

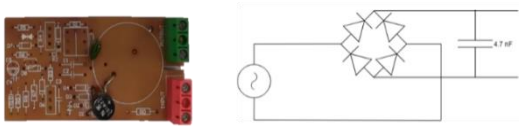

Figure 5. Rectifier.

Regarding the calibration of this type of sensors, it was necessary to optimize the excitation signal and to check for the presence of electromagnetic interference caused by other equipment in the experimental apparatus or in the laboratory. Thereby, it was necessary to define the electric signature of the AC signal in relation to the type of wave, frequency and peak-to-peak voltage, since these parameters together influence the signal/noise relationship. A square signal was used because it showed a higher read voltage value on the data acquisition board. Considering that the higher the input voltage the higher the ratio/noise, it was used a peak-to-peak voltage of 20 V because it was the maximum voltage that the signal generator could emit and that it did not endanger the board since the value did not reach the 10 V. Regarding the frequency, it was found that, since a certain frequency, the signal became saturated, reason why, after several experiments, it was found the optimal value of 2 MHz.

Commercial Sensor

As far as the commercial sensor, the sensor used was the AOGEXON model KTR-10MM, which made it possible to measure displacements up to 10 mm.

Calibration Curves

To determine the calibration curves of the displacement sensors, several incremental tests were carried out on AA1050 aluminum specimens, measuring for each increment the final height of the specimens (with the help of a digital-caliper). In other words, a relation was made between the final height of the specimens in each increment and the maximum voltage value recorded in that same increment when the press is in the lowest set point. From these results of maximum voltage, it was possible to extract the values in volts of the two displacement sensors, thus allowing to obtain the calibration curve for each of the sensors (figure 6).

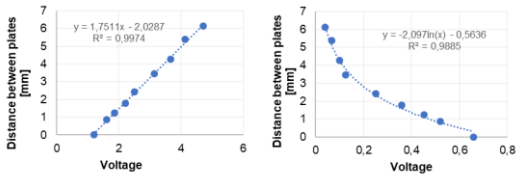

Figure 6. Calibration Curves.

Data Acquisition Board

For the data acquisition, it was used a NI-USB 6008 8-input, 12-bit data acquisition board (DAQ) with the capacity to read up to 10,000 points per second. Since these signals are characterized by a potential difference between their terminals, they were connected in differential mode, without reference to the power grid to avoid the noise coming from it. The data acquisition board alone does not have the capability to process the signals, it only receives the electrical signals and delivers a digital signal to the output. Consequently, the author developed a program in LabView Software that allows the control of the plate and the registration of the data. This program simultaneously records time, displacement and force in a "ASCII" file.

4. Materials and Methods

The materials used in the present investigation are divided into two groups: (i) pure and commercially pure metals and (ii) metal alloys. The pure metals used were: Aluminum, Zinc, Copper and Tin. In addition, two commercially pure aluminum alloys were used: AA1059 and AA1085. The metal alloy used was the AlSi9Cu3 aluminum alloy.

From the selected materials it is important to mention that the aluminum alloy AA1050 was selected with the purpose of validating the developed test tool/machine, since this material presents physical, chemical,

electrical and thermal characteristics well defined in the literature and had already been tested with different equipment in the IST, allowing to establish a comparison between its own results and the results obtained in other thesis. The remaining pure and commercially pure metals were selected since they are well defined in the literature and possess a scientific character of high importance for several engineering fields. The AlSi9Cu3 aluminum alloy was selected since it is widely used in the foundry industry on the manufacture of components for the automotive or aerospace sector, such as engine blocks.

The specimens used in the compression tests have a cylindrical shape. It is important to note that a special attention was taken in the dimensions of the specimens used, using specimens with a height/diameter ratio equal to or greater than 1, in order to reduce the influence of the friction between the faces of the specimens and the compression plates (Alves et al., 2011).

After the manufacture of the specimens, an annealing was carried out for 1:30/2:00 hours. Regarding the temperature used in the annealing of the specimens, it is the one that allows the total recrystallization of the metal. After the time mentioned above, the sample cooled slowly in the oven until it was at room temperature. It is important to note that the tin specimens do not require annealing, since it recrystallizes at room temperature (Boguslavsky et al., 2003). In the AlSi9Cu3 alloy it was also not applied any type of heat treatment since the goal for this alloy was to characterize the mechanical properties in the initial condition.

Concerning the planning of the tests, this consisted of uniaxial compression tests and hardness tests. The uniaxial compression tests were performed using the compression tool developed. These tests were performed with strain rates of 0.1 s^{-1} and 3 s^{-1}, which allowed to evaluate the influence of the strain rate on the different materials tested. In addition, the tests in which the strain rate is smaller (0.1 s^{-1}) were performed in two different conditions, in an incremental and monotonic manner, thus allowing the comparison between the flow curves with and without the contribution of the friction. Hardness tests were performed using a durometer.

5. Results and Discussion

5.1. Equipment Design and Installation

The test bench was developed in such a way that its use was as simple and intuitive as possible and that it did not present any kind of gaps or vibrations that could compromise the quality of the compression tests. In figure 7 it is possible to check the compression machine and the test bench.

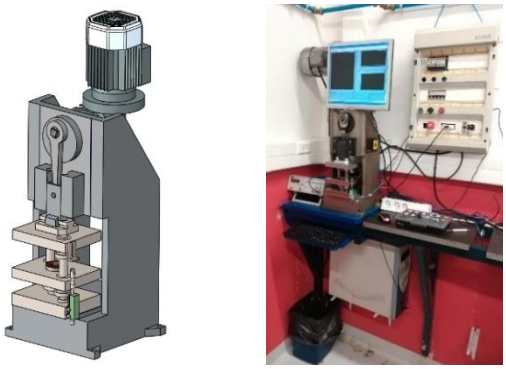

Figure 7. Experimental apparatus.

In order to validate the experimental tests, the graph stress-strain of the results of Alcino Reis (2016) and Olivier Marques (2016) was compared with the data obtained in the present investigation (see figure 8), with specimens of the same dimensions and with the same metallurgical conditions.

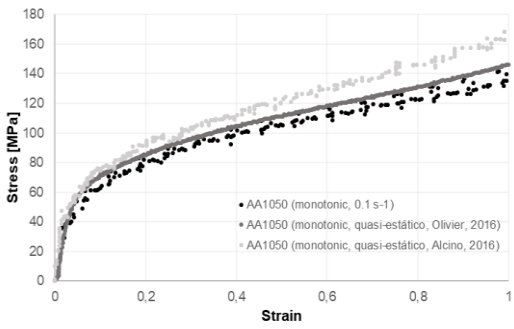

Figure 8. Comparison between curves AA1050 obtain by Olivier, Alcino and during the present work.

Figures 9 and 10 show the evolution of the force in relation with the displacement for the different materials tested. It is possible to see in Figure 9 that the two aluminum alloys (AA1050 and AA1085) have practically the same curves. This is due to the fact that, on the one hand, their physical properties are identical, and, on the other hand, the specimens used have exactly the same dimensions.

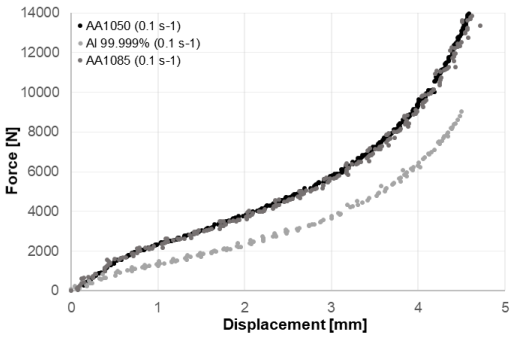

Figure 9. Force - Displacement curves for AA1050, AA1085 and Aluminium, at strain rates of up to 0.1 s^{-1}.

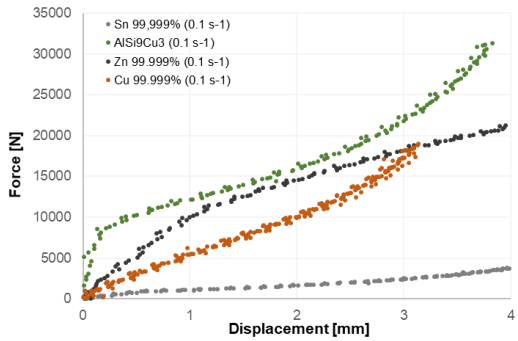

Figure 10. Force - Displacement curves for Tin, AlSi9Cu3, Zinc and Cooper, at strain rates of up to 0.1 s^{-1}.

Since the charts of the force in relation to the displacement depend on the dimensions of the specimen, these are not the ideal charts to study the mechanical behavior of the materials it is presented a set of charts of the evolution of the stress in relation to the strain (flow curves) of all the materials, whereas, unlike the graphs presented previously, these do not depend on the dimensions of the specimen. Figure 11 shows the evolution of the flow stress for pure Aluminum and the AA1050 alloy. Since the AA1085 alloy curve overlaps almost entirely with the AA1050 alloy curve (as well as the Force *vs*. Displacement curve), this is not shown. The differences shown concerning the mechanical strength between the pure aluminum and the AA1050 alloy are justified by the influence of the elements present in the metal alloy. In this sense, the elements contained in the metal alloy result in a higher flow stress than pure aluminum.

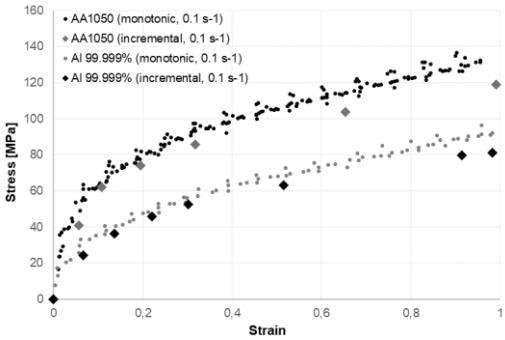

Figure 11. Flow stress - Strain curves for AA1050 and Aluminium, at strain rates of up to 0.1 s^{-1}.

Figure 12 shows the flow curves of the tested materials with higher mechanical strength. In the case of the Copper, which is a pure material, this material come up with a high mechanical resistance when compared to other pure materials tested in the present investigation.

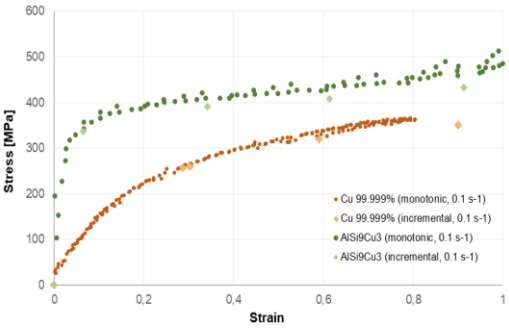

Figure 12. Flow stress - Strain curves for Copper and AlSi9Cu3, at strain rates of up to 0.1 s^{-1}.

In figure 13 it is possible to observe that Zinc and Tin show a saturation of the flow stress. This saturation is due to the fact that the recrystallization temperature of these materials is equal to, or very close to, the ambient temperature. In the case of Tin, this material is already in recrystallization at room temperature, presenting a practically constant mechanical resistance throughout

the test. In the case of zync, after a certain strain value, the mechanical resistance decreases due to the reduction of the recrystallization temperature to values close to room temperature.

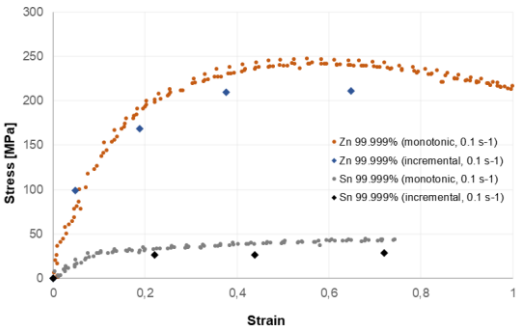

Figure 13. Flow stress - Strain curves for Zinc and Tin, at strain rates of up to 0.1 s^{-1}.

Influence of friction

During the compression test, the friction between the specimen and the plates tends to prevent the area increase at the borders of the specimen, consuming additional energy and resulting in a higher applied force. This friction effect is validated through the performance and comparison of the monotonic and incremental tests. In the incremental tests, at each increment of compression the metal particles were cleaned, and the compressor were lubricated, so has the specimen. From figures 11, 12 and 13 it is possible to observe that, for all the materials tested, when the compression tests are performed incrementally from strains of 0.3, the stress values present a significant deviation when compared to the curve of monotonic essays.

Strain Rate

Figure 14 shows the strain rate used in the present investigation. These speeds show the maximum and minimum speed that the Crank-Connecting Rod system press can achieve with values of 3 s^{-1} and 0.1 s^{-1}, respectively.

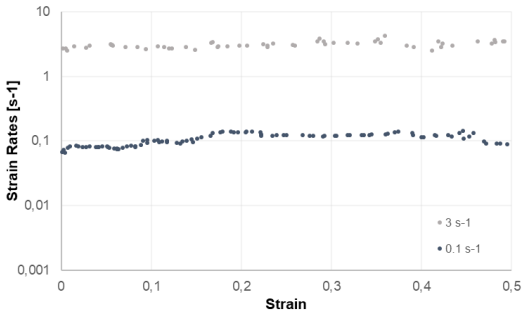

Figure 14. Strain Rates used.

Figures 15 and 16 disclose the influence of the strain rate on the flow curves of Aluminum, Copper and aluminum alloys AA1050 and AlSi9Cu3. From these figures it is possible to verify that, for pure materials (Copper and Aluminum), the flow stress increases about 5% when we increase the strain rates. In aluminum alloys, this increase in the flow stress is about 3%.

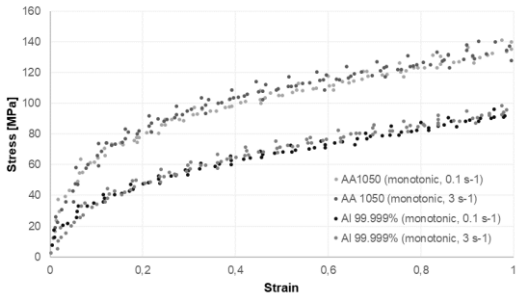

Figure 15. Flow stress - Strain curves for AA1050 and Aluminium, at diferente strain rates.

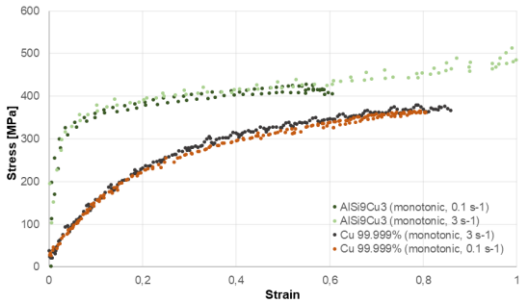

Figure 16. Flow stress - Strain curves for Copper and AlSi9Cu3, at diferente strain rates.

Figures 17 and 18 display the influence of the strain rate on the Zinc and Tin flow curves. Of all the studied materials, these are the ones that present a greater sensitivity to the strain rate, showing an increase of 18% in the case of Zinc, and 40% in the case of Tin. The higher sensitivity

presented by these materials is related to the low recrystallization temperatures they present.

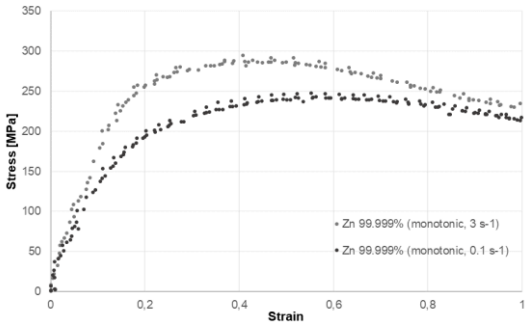

Figure 17. Flow stress - Strain curves for Zinc, at diferente strain rates.

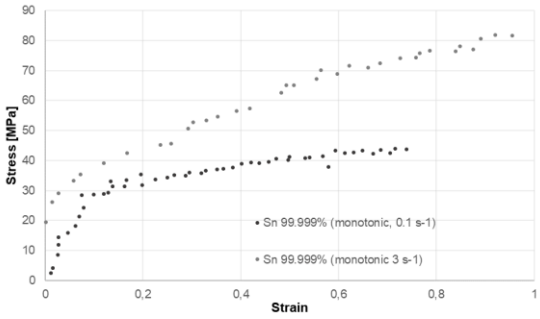

Figure 18.Flow stress - Strain curves for Tin, at diferente strain rates.

Hardness

Figures 19 and 20 show the evolution of the hardness with the flow stress of Aluminum, Copper and Aluminum alloys, AA1050, AA1085 and AlSi9Cu3. From these figures it is possible to observe that the flow stress shows a linear relationship with the hardness of the materials.

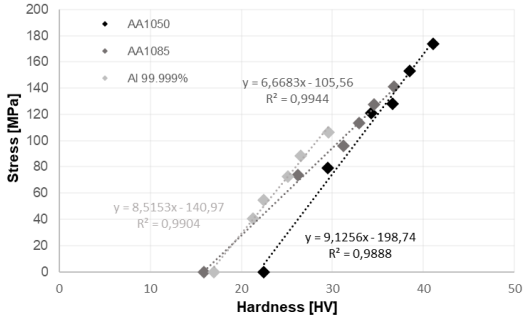

Figure 19. Stress - Hardness for AA1050, AA1085 and Aluminium.

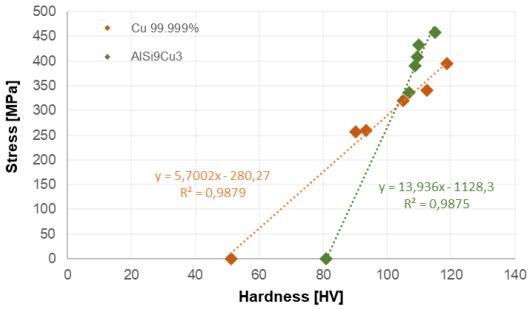

Figure 20. Stress - Hardness for Copper and AlSi9Cu3.

In materials such as Tin and Zinc, the flow stress does not show a linear relationship with the hardness of these materials since, although initially it might give the impression that this ratio is linear, as the rate of deformation increases, the hardness starts to present values very close to its initial hardness (figure 21).

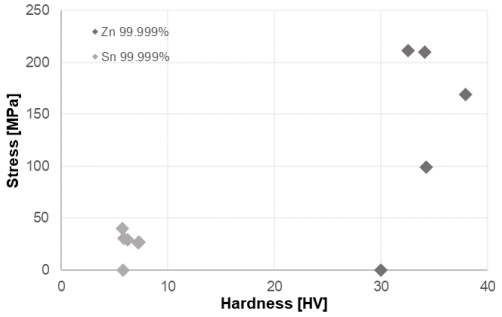

Figure 21. Stress - Hardness for Zinc and Tin.

Since, in most of the materials tested, the flow stress shows a linear relationship with the hardness of these same materials, bellow is the linear equation that relates the flow stress to the hardness:

$$\sigma(HV) = k_1 HV + k_2 \quad (6)$$

The following table 1 presents the values of k_1 and k_2 of the graph equations presented previously for the incremental tests.

Table 1. Constants of the equation 6 (0.1 s^{-1}).

Material	k_1	k_2
AA1050	9.1256	-198.74
AA1085	6.6683	-105.56
Al 99.999%	8.5153	-140.97
Cu 99.999%	5.7002	-280.27
AlSi3Cu9	13.936	-1128.3

In order to understand if the strain rate had any influence on the hardness of the materials, the initial and final hardness values were calculated for the different materials when subjected to strain rates of 3 s^{-1}. In table 2 the values of k_1 and k_2 of the equations calculated from these values are displayed.

Table 2. Constants of the equation 6 (3 s^{-1}).

Material	k_1	k_2
AA1050	9.2042	-206.71
AA1085	6.6198	-105.37
Al 99.999%	8.3608	-141.95
Cu 99.999%	5.3924	-276.2
AlSi3Cu9	12.784	-1035.5

From the observation and comparison of the equations for different strain rates, it is found that, for the same strain, the materials have a higher hardness when they are subject to higher strain rates.

6. Conclusion

From the results presented in the current investigation, it is concluded that the different materials tested display different evolutions of the stress with the strain. Regarding the hardness, from the results presented it was found that for most of the materials tested had a linear relation with the flow stress. The materials that show a different behavior have a recrystallization temperature very close to the room temperature. Regarding the influence of the strain rate on the remaining characterizing variables of the material, from the results presented it is concluded that when the strain rate is increased, the flow stress of all the materials also increases. In addition, pure metals have a higher sensitivity to strain rate than metal alloys. Finally, it is verified that, with the increase of the strain rate to the same strain, the materials have a superior hardness.

7. References

Alves, L. M., C. V. Nielsen, e P. A.F. Martins. 2011. «Revisiting the Fundamentals and Capabilities of the Stack Compression Test». *Experimental Mechanics* 51 (9): 1565–72.

Boguslavsky, Irina, e P Bush. 2003. «Recrystallization principles applied to whisker growth in tin». *APEX Conference, March*, 1–14.

Gregório, Afonso. 2017. «Ensaios de Impacto e Elevadas Velocidades de Deformação Engenharia Mecânica».

Guo, Y. B. 2003. «An integral method to determine the mechanical behavior of materials in metal cutting». *Journal of Materials Processing Technology* 142 (1): 72–81.

Lei, S., Y. C. Shin, e F. P. Incropera. 2008. «Material Constitutive Modeling Under High Strain Rates and Temperatures Through Orthogonal Machining Tests». *Journal of Manufacturing Science and Engineering* 121 (4): 577.

Marques, Olivier. 2016. «Estudo dos efeitos de escala na resistência mecânica das ligas AA1050 e AA1085». Instituto Superior Técnico.

Reis, Alcino. 2016. «Efeito de Escala na Resistência Mecânica de Materiais». Instituto Superior Técnico.